

Article

# Enamine Barbiturates and Thiobarbiturates as a New Class of Bacterial Urease Inhibitors

M. Ali <sup>1</sup>, Assem Barakat <sup>1,2,\*</sup> , Ayman El-Faham <sup>1,2,\*</sup> , Abdullah Mohammed Al-Majid <sup>1</sup>, Sammer Yousuf <sup>3</sup>, Sajda Ashraf <sup>4</sup>, Zaheer Ul-Haq <sup>4</sup> , M. Iqbal Choudhary <sup>3,4</sup>, Beatriz G. de la Torre <sup>5</sup>  and Fernando Albericio <sup>1,6,7,8</sup> 

<sup>1</sup> Department of Chemistry, College of Science, King Saud University, P.O. Box 2455, Riyadh 11451, Saudi Arabia; maly.c@ksu.edu.sa (M.A.); amajid@ksu.edu.sa (A.M.A.-M.); albericio@ub.edu (F.A.)

<sup>2</sup> Department of Chemistry, Faculty of Science, Alexandria University, P.O. Box 426, Ibrahimia, Alexandria 21321, Egypt

<sup>3</sup> Hussain Ebrahim Jamal Research Institute of Chemistry, International Center for Chemical and Biological Sciences, University of Karachi, Karachi 75270, Pakistan; dr.sammer.yousuf@gmail.com (S.Y.); iqbal.choudhary@iccs.edu (M.I.C.)

<sup>4</sup> Panjwani Center for Molecular Medicine and Drug Research, International Center for Chemical and Biological Sciences, University of Karachi, Karachi 75270, Pakistan; sajda.ashraf@yahoo.com (S.A.); zaheer\_qasmi@hotmail.com (Z.U.-H.)

<sup>5</sup> KRISP—Kwazulu-Natal Research Innovation and Sequencing Platform, College of Health Sciences, University of KwaZulu-Natal, Westville, Durban 4001, South Africa; garciadelatorreb@ukzn.ac.za

<sup>6</sup> School of Chemistry and Physics, University of KwaZulu-Natal, University Road, Westville, Durban 4001, South Africa

<sup>7</sup> Biomedical Research Networking Center in Bioengineering, Biomaterials and Nanomedicine (CIBER-BBN), Networking Centre on Bioengineering, Biomaterials and Nanomedicine, PCB, Baldiri Reixac 10, 08028 Barcelona, Spain

<sup>8</sup> Department of Organic Chemistry, University of Barcelona, Martí i Franqués 1-11, 08028 Barcelona, Spain

\* Correspondence: ambarakat@ksu.edu.sa (A.B.); aelfaham@ksu.edu.sa (A.E.-F.);

Tel.: +966-11467-5901 (A.B.); Fax: +966-11467-5992 (A.B.)

Received: 2 April 2020; Accepted: 15 May 2020; Published: 20 May 2020



**Abstract:** Urease is a therapeutic target associated with several important diseases and health problems. Based on our previous work on the inhibition of glucosidase and other enzymes and exploiting the privileged structure assigned to the (thio)barbiturate (pyrimidine) scaffold, here we tested the capacity of two (thio)barbiturate-based compound collections to inhibit urease. Several compounds showed more activity than acetohydroxamic acid as a standard tested compound. In addition, by means of a conformational study and using the Density Functional Theory (DFT) method, we identified energetically low-lying conformers. Finally, we undertook a docking study to explore the binding mechanism of these new pyrimidine derivatives as urease inhibitors.

**Keywords:** pyrimidine-trione; barbituric; thiobarbituric; urease inhibitors; DFT

## 1. Introduction

Many microorganisms use nitrogen from urease for growth (urea amidohydrolase, EC: 3.5.1.5). Urease is an enzyme that catalyzes the hydrolysis of urea into ammonia and carbon dioxide. There is a link between health complications and ammonia production by urease [1]. In animals and humans, low pH of the stomach allows microbial strains to survive, multiply, and grow, resulting in pyelonephritis, hepatic coma, gastric carcinoma, gastric lymphoma, kidney stones, and peptic ulcer complications [2,3]. The treatment of bacterial infection with therapeutics has often proven ineffective due to drug resistance. Thus, there is a clear need for alternatives or novel treatments. Given the

involvement of ureases in various diseases, pharmaceutical research has channeled considerable efforts into discovering potent and safe urease inhibitors [4–7].

Molecules with a binding site that can chelate metals are an interesting challenge and could be a promising line of action to prevent the adverse effects of ureolytic bacterial infections in humans [8]. In this regard, many types of potent urease inhibitors have been designed [9], such as dihydropyrimidines [10], urea derivatives [11], semicarbazones [12], Schiff bases [13], hydroxamic acid derivatives [14], piperazines [15], biscoumarines [16], benzimidazoles [17], and sulfonamides [18].

Enaminone molecular scaffolds have been found in many synthetic drugs and natural products [19,20]. Specially, pyrimidine-based enamines have demonstrated an array of biological activities owing to the presence of the alkenylamine moiety ( $R_2NCH=CH-$ ) in their structures, and are capable of strong bonding with metal ion chelates in biological systems [21,22].

The barbituric and thiobarbituric acids [(thio)pyrimidine trione analog derivatives] have been reported urease inhibitors [12]. These can be considered privileged structures because they have antifungal [23], antimicrobial [24,25], anti-adiponectin [26], anti-sclerosis [27], anti-convulsing [28,29], antiglycation [30], and  $\alpha$ -glucosidase inhibitory [30] properties. Several compounds **A**, **B**, and **C** have been reported, and showed anti-urease activity comparable to acetohydroxamic acid (Figure 1) [31,32].

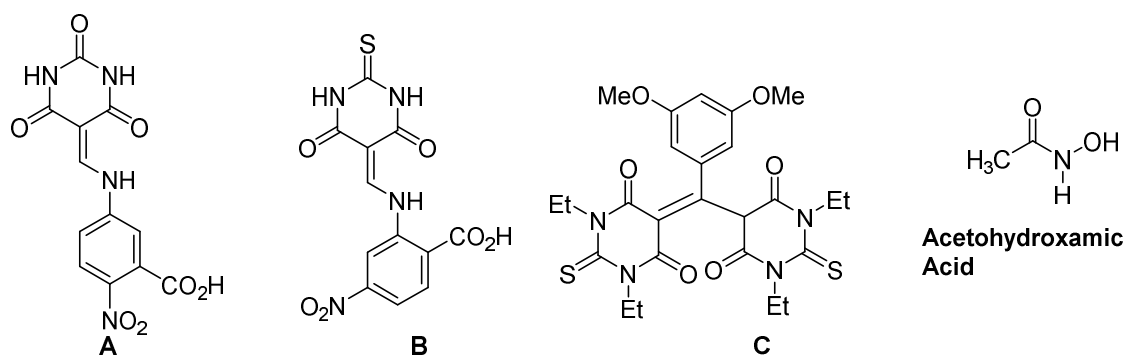


**Figure 1.** Some examples of bacterial urease inhibitors.

In this context, and as a continuation of our extended medicinal chemistry program based on the barbituric and thiobarbituric acid moieties [30,33–44], here we examined the *in vitro* anti-urease activity of a collection of 1,3-dimethylbarbiturate-enamine compounds and their analogs, thiobarbiturate derivatives. In addition, molecular docking studies were performed to evaluate the molecular interactions of the newly synthesized compounds with selected drug targets (PDB ID 4GY7).

## 2. Materials and Methods

The synthesis and the full characterization of compounds **3a**, **3d**, **3h**, **3j–p**, **4**, and **5** (Table 1) have been previously described by our group [30,33]. The rest of the compounds studied were prepared following the previously described method. The yields and full characterization are provided in the Supplementary materials.

### 2.1. *In Vitro* Urease Inhibition Assay Protocol

The urease inhibition assay was performed spectrophotometrically following the manufacturer's instructions [45–47]. The source of urease is Jack bean Urease and the full protocol provided in the supplementary materials. In the present study, urease was preincubated with the inhibitors for a period of 15 min, which proved to be sufficient in our studies.

**Table 1.** Urease inhibition capacity of compounds 3a–p, 4, and 5.

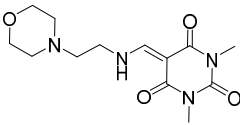
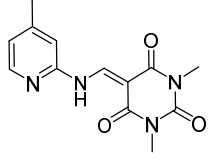
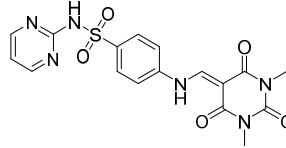
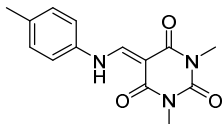
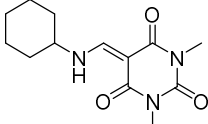
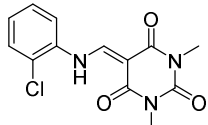
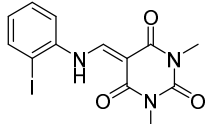
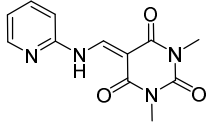
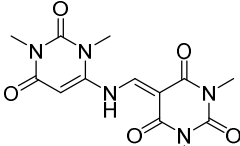
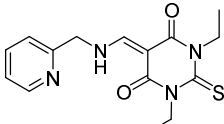
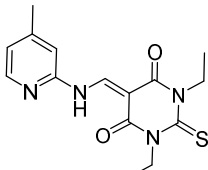
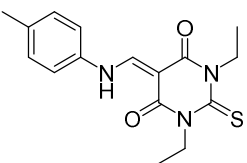
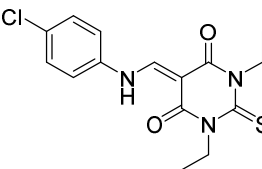
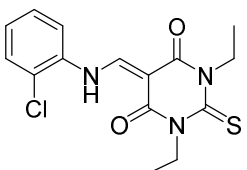
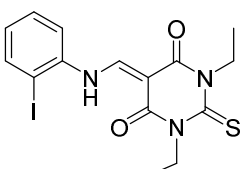
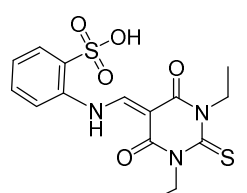
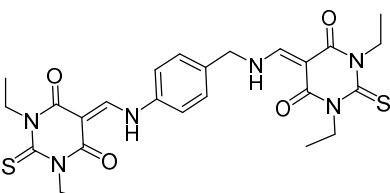
Compound	Structure	Urease Inhibition IC <sub>50</sub> ± SEM [μM]
3a		9 ± 2
3b		NA
3c		26 ± 1
3d		8 ± 0.3
3e		11 ± 0.3
3f		10 ± 0.6
3g		NA
3h		6.4 ± 0.3
3i		66 ± 2.4
3j		10 ± 0.9
3k		11 ± 1.2

Table 1. Cont.

Compound	Structure	Urease Inhibition IC <sub>50</sub> ± SEM [μM]
3l		8 ± 0.4
3m		15 ± 1.2
3n		11 ± 1.1
3o		9 ± 0.3
3p		22 ± 0.8
4		10 ± 1.2
5		42 ± 2.3
STD	Acetohydroxamic Acid (AHA)	20 ± 0.4

## 2.2. DFT Calculation

The molecular building and geometric optimization of all 18 compounds was performed by DFT using Gaussian 03W software package with basis set method B3LYP/6-31 + G(d,p). The Gauss-view program was used for molecular visualization. Geometrical, energetic and electronic parameters were calculated using structures optimized at 298 K and 1 atm. The Gibbs free energy equation ( $\Delta G = -RT \ln K$ ) was used to search conformational space.

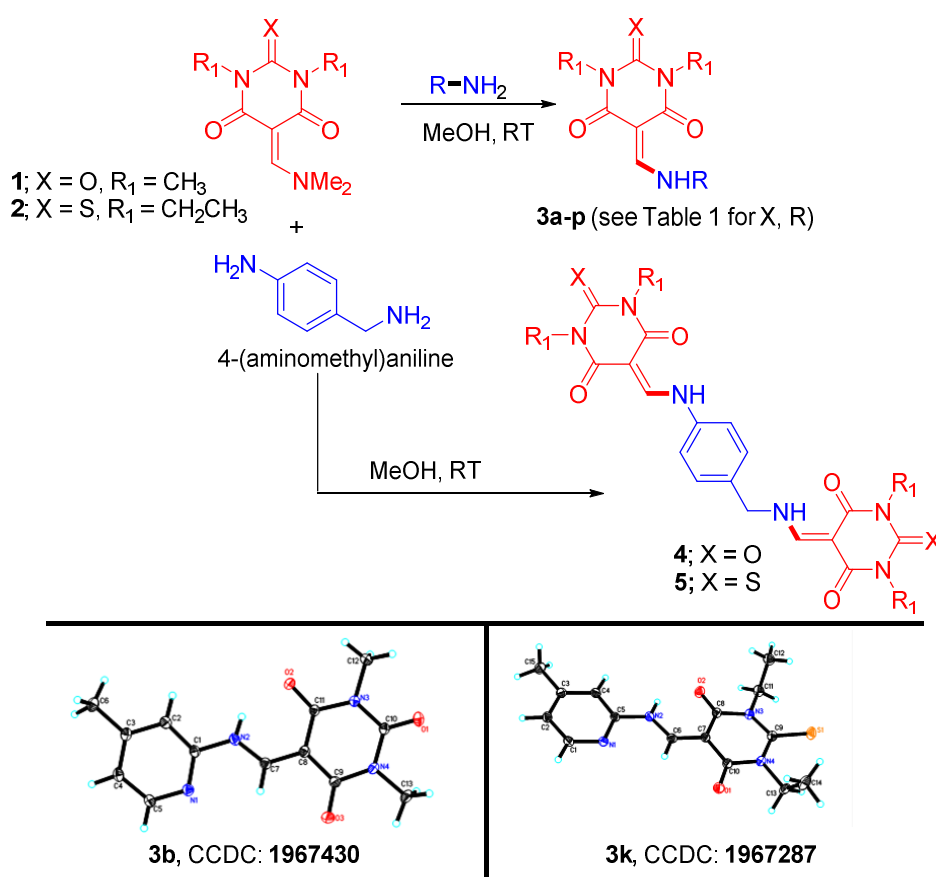
### 2.3. Molecular Docking

Molecular docking studies were conducted to rationalize the binding mode of the pyrimidine derivatives using the MOE package [Molecular Operating Environment, 2016.0810; Chemical Computing Group ULC, 1010 Sherbrooke St. West, Suite #910, Montreal, QC, Canada, H3A 2R7, 2017]. The three-dimensional structure of the urease protein was retrieved from the Protein Data Bank (PDB ID 4GY7) [48]. Water molecules were removed, and the protonation step was performed. Energy minimization using default parameters was performed to achieve a stable conformation. The optimized geometries of the pyrimidine derivatives were docked to the active site of the urease protein. For docking studies, an induced fit protocol with the triangular matcher placement method and London dG scoring function were used. The interactive docking procedure was performed for all the optimized conformers of each compound in the active site. A score was assigned to each docked compound based on its fitting in the binding cavity and its binding mode (docking study protocol are provided in the Supplementary materials).

## 3. Results and Discussion

### 3.1. Synthesis

Derivatives **3a–p**, **4**, and **5** (Table 1) were straightforwardly synthesized by nucleophilic substitution of the corresponding amines with enaminone scaffolds **1** [49] and **2** [50] in methanolic solution, following the reported method [30,33] (Scheme 1). Due to the potential tautomerism of these families of compounds, X-ray crystallography was carried out on two compounds (**3b** and **3k**) to confirm the structures. (<sup>1</sup>H-NMR and <sup>13</sup>C-NMR spectra, Figures S1–S21, and X-ray data of compounds **3b** and **3k** are provided in the Supplementary materials).



Scheme 1. Synthesis of **3a–p**, **4**, and **5**.

### 3.2. In Vitro Evaluation of Urease Inhibition

The capacity of synthesized derivatives of *N,N*-dimethylpyrimidine trione (**3a–i** and **4**) and *N,N*-diethyl-thio pyrimidine dione (**3j–p** and **5**) to inhibit urease in vitro was examined and compared with that of acetohydroxamic acid (**AHA**) ( $IC_{50} = 20 \pm 0.4 \mu M$ ), as a standard compound (Table 1).

Of note, the tested compounds showed potent urease inhibition activity, twelve of them (**3a**, **3d**, **3e**, **3f**, **3h**, **3j**, **3k**, **3l**, **3m**, **3n**, **3o**, and **4**) exerting greater activity than the reference acetohydroxamic acid. The most active member between this series is compound **3h** which the structure attributed the pyridine moiety. Separation the pyridine ring from the enaminone functionality in compound **3j** with  $CH_2$  group, the activity has been decreased compared to the most active member **3h**. On the other hands, compounds **3k**, and **3o** showed superior activity to their counterparts **3b** and **3g**. Indeed, **3l** and **3o** showed activity similar to that of **3d**, and **3f**. The chloro atom in *para*-position in compound **3m**, the activity has been decreased compared to the *ortho* position of compounds **3f**, and **3n**. Compounds **3c**, **3i** and **3p** with sulfonic, cyclic amide or sulfonamide functionalities shown less activity compared to standard drug. The cyclohexyl group in compound **3e** increases the activity with 1.8 folds than the control. It was observed that in case of compounds **4** and **5** the presence of the *N,N'*-diethyl group and the S atom in the thiobarbituric derivative **5** make them more voluminous compared to its analogs *N,N'*-dimethyl and the "O" atom in the barbituric derivatives **4**. Finally, compounds **3b**, and **3g** were not active.

However, there are some discrepancies regarding whether AHA is or is not a competitive inhibitor to the active site of the urease enzyme [51,52]. Therefore, some limitations could be applied, and we think that comparisons are important.

### 3.3. Docking Study

Molecular docking studies have the potential to identify novel drug-like molecules that display high binding affinity for the target protein, and they can facilitate the understanding of biological activity data with the purpose of designing new compounds with improved activity. Hence, we extended our study to explore the conformational space and binding orientation of the synthesized pyrimidine derivatives.

The binding conformations of these compounds were explored by MOE-Dock module implemented in the MOE program [53]. The optimized conformers obtained from the Gaussian program were docked to the active site of urease. The docking results indicated that all the conformers were well accommodated inside the active site and were stabilized by various hydrophilic, hydrophobic and van der Waals interactions. The residues involved in these interactions were Arg439, Ala440, His492, Asp494, His593, His594, Asp633 Ala636 and Met637. Compound **3h** ( $IC_{50} = 6 \pm 0.3 \mu M$ ) showed strong inhibitory potential against urease as compared to **3b** (inactive) due to methyl substitution at the *para* position of the pyridine ring. Compound **3h** showed good interactions with the residues of the active site by coordinating with the bi-nickel center, via its carbonyl group at the pyrimidine ring and anchoring itself in a way that permitted strong interaction of the carbonyl group with the two nickel ions. Additionally, the two carbonyl groups on the pyrimidine ring acted as hydrogen bond acceptors and mediated hydrogen bond interaction with His492 (2.3 Å) and Arg439 (2.04 Å) of the binding pocket (Figure 2b).

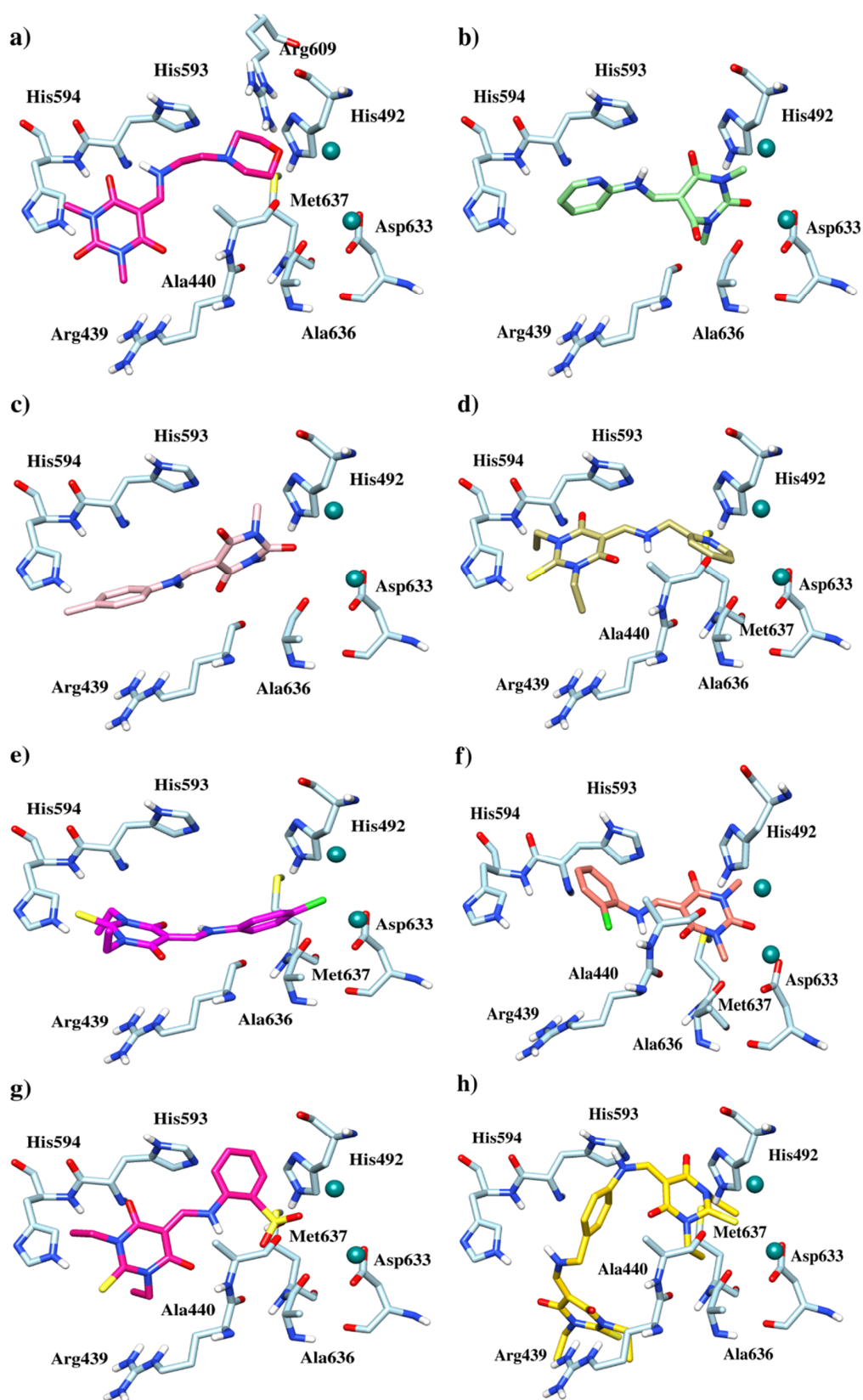


**Figure 2.** Depiction of the docking results of low energy conformer: (a) 3a, (b) 3h, (c) 3d, (d) 3j, (e) 3m, (f) 3f, (g) 3p, and (h) 5. The key residues are presented as sticks models and nickel atoms are shown as green circles.

Compound **3a** ( $IC_{50} = 9 \pm 2 \mu M$ ), another active compound of the series, established various potential interactions with the active site of urease, as well as with nickel ions. The oxygen atom of the morpholine ring was involved in the chelation process with the nickel center in the catalytic site. This compound was further stabilized by two typical hydrogen bonds with His492 (2.8 Å) and Arg609 (3.0 Å). Apart from hydrogen bond interactions, a tetramine of the compound participated in the salt bridge interaction with the negatively charged Asp494 residue (Figure 2a). Compounds **3d** and **3l** ( $IC_{50} = 8 \pm 0.3 \mu M$ ) had almost similar structures, biological activities and patterns of binding interactions with the active site residues. The only difference was the interaction with metal ions. The lone pair of electrons for sulfur ( $C = S$ ) of **3l** mediated strong interaction with the two nickel ions and hydrogen bond interaction with Arg609 (2.4 Å) and Met637 (2.8 Å), while in case of **3d**, the carbonyl group on the pyrimidine ring was involved in the interaction with the nickel ions as depicted in Figure 2c.

Compounds **3j** ( $IC_{50} = 10 \pm 0.9 \mu M$ ) and **3k** ( $IC_{50} = 11 \pm 1 \mu M$ ), which showed good biological activity, presented similar types of interactions. The additional effectiveness of **3j** compared to **3k** was due to the absence of a methyl group at the *meta* position of the benzene ring, which allowed the compound to establish close contacts with the active site residues (Figure 2d). The ring nitrogen of the pyridine is involved in two productive hydrogen bond interaction with His492 and Met637 at 2.54 and 3.4 Å, respectively. Moreover, the  $C = O$  of pyrimidine ring mediated a potential hydrogen bond interaction with the NH of His593 at 2.59 Å, while the compound was further stabilized through hydrophobic interactions with Ala440, Cme592, and His594.

The compounds with electron-withdrawing substitution, especially halogens, showed noteworthy inhibitory potential. For **3m**, **3n**, and **3o**, the presence of halogen atoms with their respective position on the benzene ring affected the binding pattern and orientation of the compound within the pocket (Figure 2e). Compounds **3f** (*o*-chloro phenyl) and **3o** (*o*-iodo phenyl) with  $IC_{50} = 10 \pm 0.6 \mu M$  showed two hydrogen bond interactions with His492 and Ala440 (Figure 2f), while **3m** and **3n** were stabilized by a single hydrogen bond with His492. These compounds also displayed hydrophobic interaction with Ala440, His593 and Met637. Compounds **3c** ( $IC_{50} = 26 \pm 1 \mu M$ ) and **3p** ( $IC_{50} = 22 \pm 0.8 \mu M$ ), both with moderate biological activity, established two hydrogen bond interactions with His492 and Ala440. However, only one interaction with the metalcenter was observed (Figure 2g). The compounds with low biological activity, as compared to the standard and other pyrimidine derivatives such as **3i** ( $IC_{50} = 66 \pm 2.4 \mu M$ ) and **5** ( $IC_{50} = 42 \pm 2.3 \mu M$ ), established single hydrogen bond interaction with the active site residue Arg439 while compound mostly established by hydrophobic interaction with the active site residues (Figure 2h). However, no interaction with nickel was observed for **3i**.

Indeed, the urease inhibition capacity of the synthesized pyrimidine derivatives is attributed to the mutual contribution of the distinct substitutions they bear. However, interaction with the metalcenter and hydrophilic interaction with Ala440, His492, His593, and Met637 are found to be crucial for the activity of these compounds.

### 3.4. Density Functional Theory (DFT)

The physicochemical properties and frontier molecular orbitals (FMOs) of the new enaminone compounds play a crucial role in enhancing bioactivity. Khon-Sham's DFT approach with the B3LYP method was used for geometry optimization [54]. The electron-donating and -withdrawing ability of a compound can be explained by its HOMO and LUMO. The higher the energy value of HOMO, the greater the electron-contributing ability of the compound. The energy difference between HOMO and LUMO is an established parameter to measure the electron conductivity or degree of intermolecular charge transfer, which also affects bioactivity [55]. In this study, to examine the urease inhibition capacity of the pyrimidine derivatives, we randomly selected compounds for comparison with DFT results.

The results of HOMO-LUMO energies were plotted against the biological activity of the pyrimidine derivatives (Table 2). Good correlation was observed between biological activity and the energies of

the LUMO orbitals. Compounds **3h**, **3k**, **3f**, and **3o** showed significant LUMO energy of  $-1.89$ ,  $-2.24$ ,  $-1.96$  and  $-2.26$  eV, respectively.

**Table 2.** Theoretical results of pyrimidine derivatives.

Compound	IC <sub>50</sub>	HOMO (eV)	LUMO (eV)	E <sub>gap</sub> (eV)
<b>3a</b>	9 ± 2	-5.79330622969	-1.21770997548	-4.57559625421
<b>3d</b>	8 ± 0.3	-5.88881823	-1.70370550982	-4.76988562237
<b>3f</b>	10 ± 0.6	-6.2202530345	-1.96248588673	-4.25776714777
<b>3h</b>	6 ± 0.3	-6.24583174683	-1.88955934518	-4.35627240165
<b>3k</b>	11 ± 1	-5.70922301574	-2.24439595033	-3.46482706541
<b>3o</b>	9 ± 0.3	-5.75357759138	-2.25963433214	-3.49394325924

The visualization of the HOMO-LUMO orbitals of **3h** reflects the localization of FMO (frontier molecular orbital) (Figure 3). The negative and positive phases of orbitals are shown in green and red, respectively. For **3h**, HOMO is localized on the pyrimidine ring, distal pyridine moiety and carbonyl group, whereas LUMO is on the pi-bond adjacent to the pyrimidine ring. In contrast, for **3o**, electrons are delocalized mainly on the benzene ring with iodine group as a substituent. The influence of LUMO energy on the inhibitory activity of the compounds might be due to the presence of halogen substitution and the pyridine ring. The halogen substitution at *ortho* and *para* positions made a great contribution to the urease inhibition capacity of the derivatives. Notably, neither HOMO nor LUMO were located on the methyl group, which would explain why this group contributed the least to binding with the protein.

The energy gap for the most active compound **3h** of the series was  $-4.35$ . A similar energy difference was observed for **3k**, **3f**, and **3o**. The smaller the difference in HOMO-LUMO energies, the greater the chemical reactivity. For any potential interaction, electron transfer from high-lying HOMO to low-lying LUMO is always energetically favorable. Given this consideration, **3h**, **3k**, **3f**, and **3o** possess good activity, which correlated well with urease inhibitory activity.

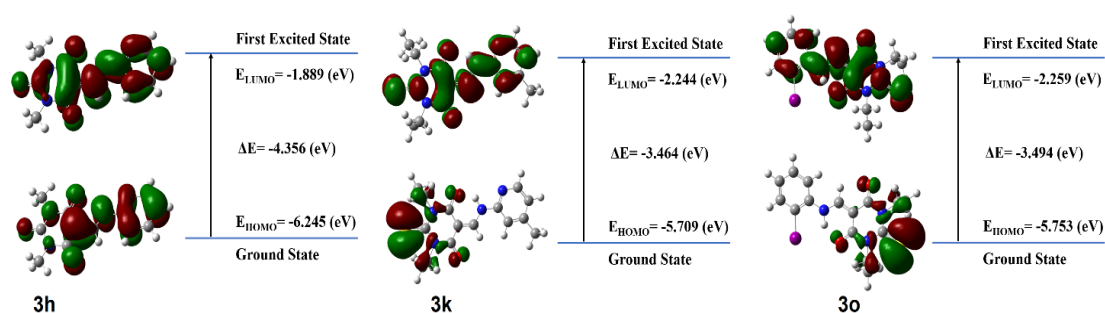


**Figure 3.** The optimized geometries and surfaces of the HOMO (Highest occupied molecular orbital)-LUMO (Lowest unoccupied molecular orbital) of **3h**, **3k** and **3o** obtained at the B3LYP/6-31G (d, p) level.

Molecular electrostatic potentials (MEP) were run for compounds **3h**, **3k**, and **3o** at B3LYP/6-31G (d, p), providing information about the sites reactive towards nucleophilic and electrophilic attack, together with hydrogen-bond interactions. The potential of electrostatic interaction at the surface is shown by blue, red and green, representing the sites for positive, negative and no electrostatic potential, respectively (Figure 4). Moreover, the positive and negative regions of the maps were responsible for the nucleophilic and electrophilic reactivity of the compounds.

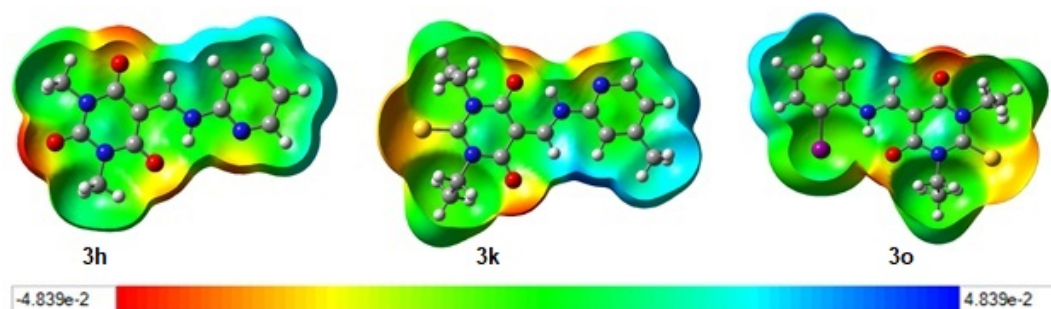


**Figure 4.** The molecular electrostatic potential (MEP) of **3h**, **3k**, and **3o**.

#### 4. Conclusions

Based on our previous work addressing the inhibition of glucosidase and taking advantage of the privileged structure associated with the (thio)barbiturate (pyrimidione) scaffold, here we have identified compounds with high in vitro anti-urease activity. All conformations of the pyrimidine derivatives were optimized with the B3LYP/6–31G method. The DFT results for the compounds correlated well with the experimental data, which indicated that the presence of the pyridine ring and electron-withdrawing groups, especially halogens (compounds **3m**, **3n**, and **3o**), play an important role in conferring urease inhibition activity. Moreover, the molecular docking studies further helped to explain the experimental results. Because of our findings, compounds **3a**, **3d**, **3h**, **3k**, and **3o** emerge as potential leads for the development of urease inhibitors. In addition, the obtained results confirm that the use of privileged structures for medicinal chemistry programs is an excellent strategy for identifying hits and leads. Further investigation will be carried out in the future for urease enzyme competitive inhibition.

**Supplementary Materials:** The following are available online at <http://www.mdpi.com/2076-3417/10/10/3523/s1>. The details of the synthesis and characterization of the studied compounds; X-ray data of compounds **3b** and **3k**; biological activity assay; docking study protocol and copies of NMR spectra (Figures S1–S21) of the synthesized target compounds are provided as Supplementary materials.

**Author Contributions:** Conceptualization, A.B. and A.E.-F.; Data curation, S.A. and Z.U.-H.; Funding acquisition, A.M.A.-M.; Investigation, M.A. and A.B.; Methodology, M.A.; Software, S.Y., S.A. and Z.U.-H.; Supervision, A.E.-F., M.I.C. and F.A.; Visualization, A.M.A.-M., M.I.C. and B.G.d.I.T.; Writing—original draft, A.B.; Writing—review & editing, A.B., M.I.C., B.G.d.I.T. and F.A. All authors have read and agreed to the published version of the manuscript.

**Funding:** Deanship of Scientific Research at King Saud University, Saudi Arabia, research group No. (RGP-044).

**Acknowledgments:** The authors would like to extend their sincere appreciation to the Deanship of Scientific Research at King Saud University for supporting and funding the research group No. (RGP-044).

**Conflicts of Interest:** The authors declare no conflict of interest.

#### References

1. Mobley, H.L.; Hausinger, R.P. Microbial ureases: Significance, regulation, and molecular characterization. *Microbiol. Mol. Biol. Rev.* **1989**, *53*, 85–108. [[CrossRef](#)]
2. Zonia, L.E.; Stebbins, N.E.; Polacco, J.C. Essential role of urease in germination of nitrogen-limited *Arabidopsis thaliana* seeds. *Plant Physiol.* **1995**, *107*, 1097–1103. [[CrossRef](#)] [[PubMed](#)]
3. Mulvaney, R.L.; Bremner, J.M. *Soil Biochemistry*; Paul, E.A., Ladd, J.N., Eds.; Marcel Dekker, Inc.: New York, NY, USA, 1981; pp. 153–196.
4. Kataria, R.; Khatkar, A. In-silico Designing, ADMET Analysis, Synthesis and Biological Evaluation of Novel Derivatives of Diosmin Against Urease Protein and *Helicobacter pylori* Bacterium. *Curr. Top. Med. Chem.* **2019**, *19*, 2658–2675. [[CrossRef](#)] [[PubMed](#)]
5. Li, W.Y.; Ni, W.W.; Ye, Y.X.; Fang, H.L.; Pan, X.M.; He, J.L.; Zhou, T.-L.; Yi, J.; Liu, S.-S.; Zhou, M.; et al. N-monoarylacethioureas as potent urease inhibitors: Synthesis, SAR, and biological evaluation. *J. Enzyme Inhib. Med. Chem.* **2020**, *35*, 404–413. [[CrossRef](#)]

6. Qamar, N.; Sultan, H.; Raheel, A.; Ashfaq, M.; Azmat, R.; Naz, R.; Raheela, L.M.; Khan, K.M.; Arshad, T. Heterochelates of metals as an effective anti-Urease agents couple with their docking studies. *Pak. J. Pharm. Sci.* **2019**, *32*, 1179–1183.
7. Shah, S.R.; Shah, Z.; Khiaat, M.; Khan, A.; Hill, L.R.; Khan, S.; Hussain, J.; Csuk, R.; Anwar, M.U.; Al-Harrasi, A. Complexes of N-and O-Donor Ligands as Potential Urease Inhibitors. *ACS Omega* **2020**, *17*, 10200–10206. [[CrossRef](#)]
8. Hanif, M.; Saleem, M.; Hussain, M.T.; Rama, N.H.; Zaib, S.; Aslam MA, M.; Iqbal, J. Synthesis, urease inhibition, antioxidant and antibacterial studies of some 4-amino-5-aryl-3H-1,2,4-triazole-3-thiones and their 3,6-disubstituted 1,2,4-triazolo[3,4-b]1,3,4-thiadiazole derivatives. *J. Braz. Chem. Soc.* **2012**, *23*, 854–860. [[CrossRef](#)]
9. Kafarski, P.; Talma, M. Recent advances in design of new urease inhibitors: A review. *J. Adv. Res.* **2018**, *13*, 101–112. [[CrossRef](#)]
10. Shamim, S.; Khan, K.M.; Salar, U.; Ali, F.; Lodhi, M.A.; Taha, M.; Perveen, S. 5-Acetyl-6-methyl-4-aryl-3,4-dihydropyrimidin-2(1H)-ones: As potent urease inhibitors; synthesis, in vitro screening, and molecular modeling study. *Bioorg. Chem.* **2018**, *76*, 37–52. [[CrossRef](#)]
11. Perveen, S.; Khan, K.M.; Lodhi, M.A.; Choudhary, M.I.; Voelter, W. Urease and  $\alpha$ -chymotrypsin inhibitory effects of selected urea derivatives. *Lett. Drug Des. Discov.* **2008**, *5*, 401–405. [[CrossRef](#)]
12. Pervez, H.; Chohan, Z.H.; Ramzan, M.; Nasim FU, H.; Khan, K.M. Synthesis and biological evaluation of some new N(4)-substituted isatin-3-thiosemicarbazones. *J. Enzyme Inhib. Med. Chem.* **2009**, *24*, 437–446. [[CrossRef](#)] [[PubMed](#)]
13. Aslam MA, S.; Mahmood, S.U.; Shahid, M.; Saeed, A.; Iqbal, J. Synthesis, biological assay in vitro and molecular docking studies of new Schiff base derivatives as potential urease inhibitors. *Eur. J. Med. Chem.* **2011**, *46*, 5473–5479. [[CrossRef](#)] [[PubMed](#)]
14. Arora, R.; Issar, U.; Kakkar, R. In silico study of the active site of Helicobacter pylori urease and its inhibition by hydroxamic acids. *J. Mol. Graph. Model.* **2018**, *83*, 64–73. [[CrossRef](#)] [[PubMed](#)]
15. Taha, M.; Wadood, A. Synthesis and molecular docking study of piperazine derivatives as potent urease inhibitors. *Bioorg. Chem.* **2018**, *78*, 411–417.
16. Khan, K.M.; Iqbal, S.; Lodhi, M.A.; Maharvi, G.M.; Choudhary, M.I.; Perveen, S. Biscoumarin: New class of urease inhibitors; economical synthesis and activity. *Bioorg. Med. Chem.* **2004**, *12*, 1963–1968. [[CrossRef](#)]
17. Menteşe, E.; Bektaş, H.; Sokmen, B.B.; Emirik, M.; Çakır, D.; Kahveci, B. Synthesis and molecular docking study of some 5,6-dichloro-2-cyclopropyl-1H-benzimidazole derivatives bearing triazole, oxadiazole, and imine functionalities as potent inhibitors of urease. *Bioorg. Med. Chem. Lett.* **2017**, *27*, 3014–3018.
18. Saeed, A.; Mahmood, S.U.; Rafiq, M.; Ashraf, Z.; Jabeen, F.; Seo, S.Y. Iminothiazoline-sulfonamide hybrids as Jack bean urease inhibitors; synthesis, kinetic mechanism and computational molecular modeling. *Chem. Biol. Drug. Des.* **2016**, *87*, 434–443. [[CrossRef](#)]
19. Mabkhot, Y.N.; Barakat, A.; Yousuf, S. Substituted thieno [2, 3-b] thiophenes and related congeners: Synthesis,  $\beta$ -glucuronidase inhibition activity, crystal structure, and POM analyses. *Bioorg. Med. Chem.* **2014**, *22*, 6715–6725. [[CrossRef](#)]
20. Mabkhot, Y.N.; Al-Majid, A.M.; Barakat, A.; Alshahrani, S.; Siddiqui, Y. 1, 1'-(3-Methyl-4-phenylthieno [2-b] thiophene-2, 5-diyl) diethanone as a building block in heterocyclic synthesis. novel synthesis of some pyrazole and pyrimidine derivatives. *Molecules* **2011**, *16*, 6502–6511. [[CrossRef](#)]
21. Fırıncı, R.; Fırıncı, E.; Başbülbul, G.; Dabanca, M.B.; Celepci, D.B.; Günay, M.E. Enamines of 1, 3-dimethylbarbiturates and their symmetrical palladium (II) complexes: Synthesis, characterization and biological activity. *Trans. Met. Chem.* **2019**, *44*, 391–397.
22. Cox, D.S.; Scott, K.R.; Gao, H.; Eddington, N.D. Effect of P-glycoprotein on the pharmacokinetics and tissue distribution of enaminone anticonvulsants: Analysis by population and physiological approaches. *J. Pharmacol. Exp. Ther.* **2002**, *302*, 1096–1104. [[CrossRef](#)] [[PubMed](#)]
23. Kidwai, M.; Thakur, R.; Mohan, R. Ecofriendly synthesis of novel antifungal (thio)- barbituric acid derivatives. *Acta Chim. Solv.* **2005**, *52*, 88–92.
24. Figueiredo, J.; Serrano, J.L.; Cavalheiro, E.; Keurulainen, L.; Yli-Kauhaluoma, J.; Moreira, V.M.; Almeida, P. Trisubstituted barbiturates and thiobarbiturates: Synthesis and biological evaluation as xanthine oxidase inhibitors, antioxidants, antibacterial and anti-proliferative agents. *Eur. J. Med. Chem.* **2018**, *143*, 829–842. [[CrossRef](#)] [[PubMed](#)]

25. Dabholkar, V.V.; Ravi, T.D. Synthesis of Biginelli products of thiobarbituric acids and their antimicrobial activity. *J. Serb. Chem. Soc.* **2010**, *75*, 1033–1040. [[CrossRef](#)]
26. Ma, L.; Li, S.; Zheng, H. Synthesis and biological activity of novel barbituric and thiobarbituric acid derivatives against non-alcoholic fatty liver disease. *Eur. J. Med. Chem.* **2011**, *46*, 2003. [[CrossRef](#)] [[PubMed](#)]
27. Khan, K.M.; Ali, M.; Farooqui, T.A.; Khan, M.; Taha, M.; Perveen, S. An improved method for the synthesis of 5- arylidene barbiturates using BiCl<sub>3</sub>. *J. Chem. Soc. Pak.* **2009**, *31*, 823–828.
28. Archana, S.V.K.; Kumar, A. Synthesis of some newer derivatives of substitute quinazolinonyl-2-oxo/thiobarbituric acid as potent anticonvulsant agents. *Bioorg. Med. Chem.* **2004**, *12*, 1257–1264. [[CrossRef](#)]
29. Hassan, M.; Khan Faidallah, K.A. Synthesis and biological evaluation of new barbituric and thiobarbituric acid fluoro analogs of benzenesulfonamides as antidiabetic and antibacterial agents. *J. Fluorine Chem.* **2012**, *142*, 96–104.
30. Ali, M.; Barakat, A.; El-Faham, A.; Al-Rasheed, H.H.; Dahlous, K.; Al-Majid, A.M.; Choudhary, M.I. Synthesis and characterisation of thiobarbituric acid enamine derivatives, and evaluation of their  $\alpha$ -glucosidase inhibitory and anti-glycation activity. *Enzyme Inhib. Med. Chem.* **2020**, *35*, 692–701. [[CrossRef](#)]
31. Puerta, D.T.; Cohen, S.M.A. A bioinorganic perspective on matrix metalloproteinase inhibition. *Curr. Topic. Med. Chem.* **2004**, *4*, 1551–1573. [[CrossRef](#)]
32. Hameed, A.; Al-Rashida, M.; Uroos, M. A patent update on therapeutic applications of urease inhibitors (2012–2018). *Expert Opin. Rapeut. Pat.* **2019**, *29*, 181–189. [[CrossRef](#)] [[PubMed](#)]
33. Barakat, A.; Soliman, S.M.; Ali, M.; Elmarghany, A.; Al-Majid, A.M.; Yousuf, S.; El-Faham, A. Synthesis, crystal structure, evaluation of urease inhibition potential and the docking studies of cobalt(III) complex based on barbituric acid Schiff base ligand. *Inorg. Chim. Acta.* **2020**, *503*, 119405. [[CrossRef](#)]
34. Barakat, A.; Ali, M.; Al-Majid, A.M.; Yousuf, S.; Choudhary, M.I.; Khalil, R.; Ul-Haq, Z. Synthesis of thiobarbituric acid derivatives: In vitro  $\alpha$ -glucosidase inhibition and molecular docking studies. *Bioorg. Chem.* **2017**, *75*, 99–105. [[CrossRef](#)] [[PubMed](#)]
35. Barakat, A.; Al-Majid, A.M.; Al-Najjar, H.J.; Mabkhot, Y.N.; Javaid, S.; Yousuf, S.; Choudhary, M.I. Zwitterionic pyrimidinium adducts as antioxidants with therapeutic potential as nitric oxide scavenger. *Eur. J. Med. Chem.* **2014**, *84*, 146. [[CrossRef](#)] [[PubMed](#)]
36. Barakat, A.; Islam, M.S.; Al-Majid, A.M.; Ghabbour, H.A.; Fun, H.K.; Javed, K.; Wadood, A. Synthesis, in vitro biological activities and in silico study of dihydropyrimidines derivatives. *Bioorg. Med. Chem.* **2015**, *23*, 6740. [[CrossRef](#)] [[PubMed](#)]
37. Barakat, A.; Al-Majid, A.M.; Soliman, S.M.; Lotfy, G.; Ghabbour, H.A.; Fun, H.K.; Sloop, J.C. New diethyl ammonium salt of thiobarbituric acid derivative: Synthesis, molecular structure investigations and docking studies. *Molecules* **2015**, *20*, 20642–20658. [[CrossRef](#)] [[PubMed](#)]
38. Barakat, A.; Al-Majid, A.M.; Lotfy, G.; Arshad, F.; Yousuf, S.; Choudhary, M.I.; Ul-Haq, Z. Synthesis and Dynamics Studies of Barbituric Acid Derivatives as Urease Inhibitors. *Chem. Cent. J.* **2015**, *9*, 63. [[CrossRef](#)]
39. Badria, F.A.; Atef, S.; Al-Majid, A.M.; Ali, M.; Elshaier, Y.A.; Ghabbour, H.A.; Barakat, A. Synthesis and inhibitory effect of some indole-pyrimidine-based hybrid heterocycles on  $\alpha$ -glucosidase and  $\alpha$ -amylase as potential hypoglycemic agents. *ChemistryOpen* **2019**, *8*, 1288–1297. [[CrossRef](#)]
40. Barakat, A.; Islam, M.S.; Al-Majid, A.M.; Ghabbour, H.A.; Yousuf, S.; Ashraf, M.; Ul-Haq, Z. Synthesis of pyrimidine-2,4,6-trione derivatives: Anti-oxidant, Anti-cancer,  $\alpha$ -glucosidase,  $\beta$ -glucuronidase inhibitor and their molecular docking studies. *Bioorg. Chem.* **2016**, *86*, 72–79. [[CrossRef](#)]
41. Barakat, A.; Soliman, S.M.; Elshaier, Y.A.M.M. Molecular structure investigation, hypoglycemic/anticancer and docking studies of 5-((4-fluorophenyl)(2-hydroxy-6-oxocyclohex-1-en-1-yl)methyl)-6-hydroxy-1,3-dimethylpyrimidine-2,4(1H,3H)-dione. *J. Mol. Struc.* **2017**, *1134*, 99–111. [[CrossRef](#)]
42. Ul-Haq, Z.; Ashraf, S.; Al-Majid, A.M.; Barakat, A. 3D-QSAR Studies on Barbituric Acid Derivatives as Urease Inhibitors and the Effect of Charges on the Quality of a Model. *Int. J. Mol. Sci.* **2016**, *17*, 657. [[CrossRef](#)] [[PubMed](#)]
43. Khan, K.M.; Rahim, F.; Khan, A. Synthesis and structure–activity relationship of thiobarbituric acid derivatives as potent inhibitors of urease. *Bioorg. Med. Chem.* **2014**, *22*, 4119. [[CrossRef](#)] [[PubMed](#)]
44. Altowyan, M.S.; Barakat, A.; Soliman, S.M.; Al-Majid, A.M.; Ali, M.; Elshaier, Y.A.; Ghabbour, H.A. A New Barbituric Acid Derivatives as Reactive Oxygen Scavenger: Experimental and Theoretical Investigations. *J. Mol. Struc.* **2019**, *1175*, 524–535. [[CrossRef](#)]

45. Weatherburn, M.W. Phenol-hypochlorite reaction for determination of ammonia. *Anal. Chem.* **1967**, *39*, 971. [[CrossRef](#)]
46. Mabkhot, Y.N.; Aldawsari, F.D.; Al-Showiman, S.S.; Barakat, A.; Soliman, S.M.; Choudhary, M.I.; Hadda, T.B. Novel enaminone derived from thieno [2-b] thiene: Synthesis, x-ray crystal structure, HOMO, LUMO, NBO analyses and biological activity. *Chem. Cent. J.* **2015**, *9*, 24. [[CrossRef](#)]
47. Khan, M.K.; Saify, Z.S.; Arif Lodhi, M.; Butt, N.; Perveen, S.; Murtaza Maharvi, G.; Atta-Ur-Rahman. Piperidines: A new class of urease inhibitors. *Nat. Prod. Res.* **2006**, *20*, 523. [[CrossRef](#)]
48. Begum, A.; Banumathi, S.; Choudhary, M.I.; Betzel, C. Crystallographic structure analysis of urease from Jack bean (*Canavalia ensiformis*) at 1.49 Å Resolution. *Macromolecules* **2012**. [[CrossRef](#)]
49. Kulinich, A.V.; Derevyanko, N.A.; Ishchenko, A.A. Synthesis and spectral properties of cyanine dyes-derivatives of 10,10-dimethyl-7,8,9,10-tetrahydro-6H-pyrido[1-a]indolium. *J. Photochem. Photobiol.* **2008**, *198*, 119–125. [[CrossRef](#)]
50. Gorobets, N.Y.; Yousefi, B.H.; Belaj, F.; Kappe, C.O. Rapid microwave-assisted solution phase synthesis of substituted 2-pyridone libraries. *Tetrahedron* **2004**, *60*, 8633–8644. [[CrossRef](#)]
51. Kumar, S.; Kayastha, A.M. Acetohydroxamic Acid—A Competitive Inhibitor of Urease from Soybean “Glycine max”. *J. Proteins Proteom.* **2013**, *1*, 3–8.
52. Krajewska, B.; Zaborska, W. Jack bean urease: The effect of active-site binding inhibitors on the reactivity of enzyme thiol groups. *Bioorg. Chem.* **2007**, *35*, 355–365. [[CrossRef](#)] [[PubMed](#)]
53. Chemical Computing Group. *Molecular Operating Environment (MOE) 2016.0810*; Chemical Computing Group Inc.: Montreal, QC, Canada, 2016. Available online: <https://www.chemcomp.com/Products.htm> (accessed on 19 May 2020).
54. Rauf, A.; Shahzad, S.; Bajda, M.; Yar, M.; Ahmed, F.; Hussain, N.; Jończyk, J. Design and synthesis of new barbituric-and thiobarbituric acid derivatives as potent urease inhibitors: Structure activity relationship and molecular modeling studies. *Bioorg. Med. Chem.* **2015**, *23*, 6049–6058. [[CrossRef](#)] [[PubMed](#)]
55. Stephens, P.J.; Devlin, F.J.; Chabalowski, C.F.N.; Frisch, M.J. Ab initio calculation of vibrational absorption and circular dichroism spectra using density functional force fields. *J. Phys. Chem.* **1994**, *98*, 11623–11627. [[CrossRef](#)]



© 2020 by the authors. Licensee MDPI, Basel, Switzerland. This article is an open access article distributed under the terms and conditions of the Creative Commons Attribution (CC BY) license (<http://creativecommons.org/licenses/by/4.0/>).